Scientific Reports

https://doi.org/10.1038/s41598-026-50905-4

Article in Press

Autonomic impairment in advanced heart-failure patients revealed by nonlinear heart rate variability measured during exercise

Received: 23 December 2025

Accepted: 24 April 2026

Published online: 10 June 2026

Cite this article as: Castelbuono S., Bellavia D., Sparacino L. *et al.* Autonomic impairment in advanced heart-failure patients revealed by nonlinear heart rate variability measured during exercise. *Sci Rep* (2026). https://doi.org/10.1038/s41598-026-50905-4

Salvatore Castelbuono, Diego Bellavia, Laura Sparacino, Yuri Antonacci, Riccardo Pernice, Eluisa La Franca, Vincenzo Nuzzi, Paolo Manca, Filippo Bova, Valentina Agnese, Manlio Cipriani & Luca Faes

Autonomic Impairment in Advanced Heart-Failure Patients Revealed by Nonlinear Heart Rate Variability Measured during Exercise

Salvatore Castelbuono[1,2*], Diego Bellavia[1], Laura Sparacino[2], Yuri Antonacci[2], Riccardo Pernice[2], Eluisa La Franca[1,3], Vincenzo Nuzzi[1,3], Paolo Manca[1,3], Filippo Bova[4], Valentina Agnese[1], Manlio Cipriani[1,3], and Luca Faes[2]

[1]IRCCS ISMETT, Palermo, Italy
[2]Department of Engineering, University of Palermo, Palermo, Italy
[3]UPMC Italy, Palermo, Italy
[4]Department of Experimental and Clinical Medicine, Magna Graecia University, Catanzaro, Italy
[*]scastelbuono@ismett.edu

ABSTRACT

Advanced heart failure is characterized by profound autonomic dysfunction, yet resting measures of heart rate variability (HRV) provide limited insight into autonomic adaptability under physiological stress. We investigated whether graded exercise unmasks alterations in cardiac autonomic regulation in patients with advanced heart failure using both conventional and information-theoretic HRV measures. 77 patients with end-stage heart failure with reduced ejection fraction underwent resting and cycle-ergometer exercise testing with continuous electrocardiographic recording. HRV was assessed at rest, during early exercise and at peak exercise using time- and frequency-domain indices alongside entropy-based measures of cardiac rhythm complexity. Clinical follow-up was performed for a composite adverse outcome, defined as cardiovascular death, comprising cardiac-related death, heart transplantation or left ventricular assist device implantation. During graded exercise, conventional HRV measures showed the expected workload-dependent attenuation, whereas entropy-based metrics revealed a progressive increase in signal complexity and a reduction in heartbeat predictability. Notably, during the early phase of exercise, patients who subsequently experienced adverse outcomes (n=17) exhibited lower conditional entropy and higher self-entropy compared with survivors, while no differences were observed at rest or peak exercise. In survival analyses, self-entropy measured during early exercise remained independently associated with adverse outcomes after adjustment for clinical and exercise-derived variables. These findings indicate that early exercise represents a sensitive physiological window for revealing impaired autonomic adaptability in advanced heart failure. Information-theoretic analysis of HRV during submaximal exercise may provide complementary insights into cardiac autonomic regulation that are not captured by conventional resting or peak exercise measures.

1 Introduction

Heart failure with reduced ejection fraction (HFrEF) remains a major global health challenge, affecting tens of millions of individuals worldwide and accounting for substantial morbidity, mortality and healthcare expenditure[1,2]. Despite advances in pharmacological and device-based therapies, outcomes remain poor, particularly in advanced stages of disease. HFrEF is characterized by impaired left ventricular contractility and chronic autonomic imbalance, marked by excessive sympathetic activation and blunted parasympathetic modulation[3]. This dysregulation contributes to arrhythmogenesis, exercise intolerance, and adverse prognosis, with five-year post-hospitalization survival rates reported as low as 25%[4].

HFrEF patients represent a vulnerable population, with profound autonomic dysregulation, limited cardiac reserve and high arrhythmic risk. Heart rate variability (HRV) is a widely used, non-invasive marker of cardiac autonomic regulation and cardiovascular adaptability[5,6]. In HFrEF, reduced HRV has been consistently associated with hospitalization, arrhythmic events and mortality, often outperforming conventional clinical markers such as left ventricular ejection fraction or cardiac index[7,8]. However, most evidence supporting the prognostic value of HRV has been derived from resting recordings, which may not adequately reflect autonomic responsiveness under physiological stress.

Exercise represents a clinically relevant perturbation of cardiovascular control and provides insight into dynamic autonomic regulation. During graded exercise, heart rate acceleration is initially mediated by parasympathetic withdrawal and subsequently by increasing sympathetic activation[9]. In healthy individuals, increasing workload is typically associated with a reduction in HRV complexity, reflecting sinus node regularization under sympathetic predominance[9,10]. In contrast, in patients with HFrEF,

this physiological transition is often disrupted; the inability to effectively withdraw residual vagal tone or mount an adequate sympathetic response leads to chronotropic incompetence. This blunted heart rate response not only constrains cardiac output and increases reliance on stroke volume, contributing to reduced exercise tolerance, but also results in altered beat-to-beat dynamics where the expected transition to a regularized, sympathetically driven rhythm is delayed or fragmented[11]. These abnormalities may impair the ability of conventional HRV metrics assessed at rest or peak exertion to capture subtle deficits in autonomic adaptability.

Traditional time- and frequency-domain HRV measures primarily quantify the magnitude of heart rate fluctuations and are based on linear assumptions[5,6]. While these indices provide valuable information, they may not fully characterize the structural organization and predictability of cardiac rhythm regulation, particularly under non-stationary conditions such as exercise. In HFrEF and during physical exertion, the drastic reduction in variability amplitude and the presence of exercise-induced tachycardia further limit the reliability of linear indices in reflecting autonomic modulation[12]. Entropy-based HRV metrics extend conventional analysis by quantifying the complexity and unpredictability of beat-to-beat dynamics. Unlike other nonlinear methods that measure correlation properties, entropy-based indices provide a direct measure of the information dynamics and the degree of coupling within the cardiovascular control system, thereby offering insight into the quality and flexibility of autonomic control rather than variability amplitude alone[13–15]. A significant advantage of these measures is their model-free nature, which enables the detection of nonlinearity without the constraints of specific structural assumptions inherent in model-based approaches[16]. Altered entropy has been associated with disease severity and adverse outcomes in heart failure and other cardiovascular conditions[17–19]. In addition, surrogate-data analysis allows discrimination between genuine nonlinear physiological structure and stochastic variability, enabling more robust identification of pathological autonomic regulation and workload-dependent changes in cardiac rhythm dynamics[20–22].

Despite these advances, few studies have examined nonlinear HRV dynamics and entropy-based complexity during exercise in patients with end-stage HFrEF, with most investigations focusing on resting conditions or stable ambulatory populations[23]. Previous research using fractal-based nonlinear metrics, such as detrended fluctuation analysis (DFA), has demonstrated that scaling exponents are sensitive to exercise intensity and can be used to identify physiological thresholds in patients with chronic heart failure[24]. However, reliable estimation of long-range scaling exponents (DFA-alpha2) requires longer recordings, and even short-term exponents (DFA-alpha1) reflect a single correlation property[25] rather than the multidimensional characterization of complexity and predictability afforded by information-theoretic measures. Indeed, the measures of conditional entropy and information storage employed in this study are optimized for shorter time series[15,17], making them particularly suitable for capturing the rapid short-term cardiovascular interactions that occur during the transitions of a graded exercise test. In particular, the early phase of exercise, representing a transitional state of autonomic reorganization, remains poorly explored, despite its potential to unmask latent autonomic vulnerability that may not be evident at rest or during maximal exertion.

Accordingly, the aim of this study was to characterize autonomic regulation in transplant-listed patients with advanced HFrEF by analyzing HRV dynamics at rest and during graded exercise, with particular emphasis on the early exercise phase. By integrating conventional time- and frequency-domain HRV measures with entropy-based indices of cardiac rhythm complexity, we sought to characterize workload-dependent changes in cardiac rhythm dynamics and to determine whether autonomic responses to submaximal physiological stress are associated with adverse cardiovascular outcomes, providing incremental prognostic information beyond established clinical and exercise-derived parameters.

2 Methods

2.1 Patient Cohort

The study cohort was drawn from the IRCCS ISMETT Heart Failure Registry. Patient enrollment occurred between June 1st, 2023 and March 31st, 2025, and follow-up was completed on November 30th, 2025. During this period, 160 patients were evaluated. Inclusion criteria were age $\geq$ 18 years and left ventricular ejection fraction (LVEF) $\leq$ 40%, as assessed by two-dimensional echocardiography. Of the 160 patients initially evaluated, 27 were excluded prior to signal acquisition due to clinical instability, absolute contraindications to exercise testing, or withdrawal of consent; the remaining 133 underwent the acquisition protocol. After acquisition, recordings were screened for quality control. Patients were excluded from the final analysis if they did not successfully complete the exercise test (n=4), if less than 3 minutes of resting electrocardiographic (ECG) recording were available (n=10), or if ECG signals showed unacceptable quality due to excessive noise or artifacts (n=42), including frequent ventricular ectopy and predominant pacemaker-driven rhythm. The study was approved by the IRCCS ISMETT's Institutional Research Review Board and the relevant local ethics committee (project number: IRRB/08/24). All patients provided written informed consent prior to participation. All methods were carried out in accordance with relevant guidelines and regulations and in compliance with the principles of the Declaration of Helsinki and its later amendments.

A total of 77 patients ultimately met eligibility criteria and were included in the final study sample (mean age 49.70 $\pm$ 13.07 years; 58 males and 19 females). All participants were listed for heart transplantation for end-stage HFrEF. Heart failure etiology was ischemic (IHF) in 32 patients (41.56%) and non-ischemic (NIHF) in 45 patients (58.44%). To ensure robustness against

potential confounding, comprehensive demographic and clinical data were collected at baseline, including: age, sex, weight, Body Mass Index (BMI), New York Heart Association (NYHA) functional class, systolic (SBP) and diastolic blood pressure (DBP), and Left Ventricular Ejection Fraction (LVEF). Data regarding the presence of cardioverter-defibrillator (ICD)/cardiac resynchronization therapy (CRT) and current pharmacological therapies were also recorded to characterize the specialized nature of the study population. Specifically, among the 77 subjects, 53 (68.83%) had an implantable ICD and 12 (15.58%) had a CRT device at the time of the study. Pharmacological treatment at the time of evaluation included β-blockers in 73 patients (94.81%), angiotensin-converting enzyme (ACE) inhibitors in 16 (20.78%), angiotensin receptor-neprilysin inhibitors (ARNI) in 46 (59.74%), mineralocorticoid receptor antagonists (MRA) in 67 (87.01%), diuretics in 57 (74.03%), sodium-glucose co-transporter 2 (SGLT2) inhibitors in 65 (84.41%).

During the study period, 17 patients experienced an adverse clinical outcome defined as *cardiovascular death* (D), which encompassed cardiac-related death (n=2), heart transplantation (n=7) or implantation of a left ventricular assist device (LVAD; n=8). The remaining 60 participants were classified as *surviving* subjects (S). The median follow-up duration was 377 days (IQR: 275–550 days), with all participants censored at the end of the study or at the occurrence of the composite endpoint.

2.2 Signal Acquisition and Time Series Extraction

ECG recordings were acquired using a PC-ECG 1200 system (Wireless 12-Lead ECG, NORAV Medical, Germany), configured in a standard 12-lead setup with a sampling rate of 500 Hz. Data acquisition was performed continuously across two distinct phases: a resting baseline and a graded exercise test. During the resting phase, participants remained seated while ECG signals were recorded to establish baseline cardiac activity for at least 3 minutes. Subsequently, participants completed a graded exercise test on a calibrated cycle-ergometer following a ramp protocol[26], in which workload was progressively increased to elicit a gradual cardiovascular response without a warm-up phase. The ramp profile was individually adjusted based on each participant's age, fitness level and clinical condition to ensure that the total duration of the exercise session was approximately 10 ± 2 minutes and could be completed without premature fatigue. The ramp increment ranged between 5 and 15 $Watts/min$, in accordance with standard recommendations for heart failure populations[27]. Maximal exercise tolerance was determined by the patient's refusal or inability to maintain the prescribed cycling cadence or the onset of clinical symptoms. Respiratory gas exchange was measured breath-by-breath using a metabolic cart (Vyntus CPX, Vyaire Medical, Germany). The system employs fast-response oxygen and carbon dioxide analyzers to continuously measure oxygen uptake ($\dot{V}O_2$), carbon dioxide production ($\dot{V}CO_2$) and ventilatory parameters during exercise. Peak oxygen uptake ($\dot{V}O_2$peak) was defined as the highest 30 seconds averaged value of oxygen uptake achieved during the test. Ventilatory efficiency ($\dot{V}E/\dot{V}CO_2$ slope) was quantified by the slope of the relationship between minute ventilation and carbon dioxide production.

All signal preprocessing and HRV analyses were performed in MATLAB (version R2025b, MathWorks, Natick, MA, USA) using custom-developed scripts based on previous developed software[28]. For each subject, the raw ECG signal was processed using a 4th-order band-pass Butterworth filter with a lower cutoff frequency of 0.5 Hz to remove baseline wander and an upper cutoff of 40 Hz to attenuate high-frequency noise, including electromyographic activity and power-line interference. From the filtered ECG signals, physiological time series representing the dynamic activity of heart beat variability were extracted. First, R-peaks of the ECG were detected using the Pan-Tompkins algorithm[29] and all detections were visually inspected. To preserve the integrity of the heartbeat dynamics analysis, only recordings in which corrected ectopic beats accounted for less than 5% of the total segment were included. Manual corrections were applied in case of false or missed detections and ectopic beats within these limits were replaced using cubic spline interpolation. For patients with ICD or CRT devices, analysis focused exclusively on segments of intrinsic sinus rhythm; any segments containing paced beats were excluded to prevent artifactual distortion of HRV metrics. Patients with excessive noise or poor signal quality in their recordings were excluded to ensure the reliability of the HRV estimates.

R-R interval time series, defined as the time intervals between consecutive R-peaks, were then derived. Segments containing 150 consecutive heartbeats were selected from the R-R interval time series during the resting state condition, while two segments of 300 beats were extracted to represent the early (first 300 beats of the series) and late (last 300 beats) stages of the workload period. Consequently, three conditions were analyzed and compared: *Rest*, *Early* exercise and *Late* exercise. To avoid excluding subjects with shorter resting recordings while maintaining sufficient data for HRV estimation, a segment length of 150 beats was selected for resting analyses. Importantly, previous studies have demonstrated that short-term HRV metrics can be reliably estimated from as few as 120 samples[30–32], and these measures are sensitive enough to discern clinical and pathophysiological states[33]. During exercise, the progressive increase in heart rate and the dynamic physiological adjustments introduce greater non-stationarity in the R–R interval series. To improve the robustness of HRV estimation under these conditions, a longer window of 300 beats was used for the exercise stages. This choice is consistent with recommendations suggesting that longer segments provide more stable estimates for frequency-domain and entropy-based HRV measures, particularly when the signal exhibits time-varying characteristics[5,6].

2.3 Assessment of Heart Rate Variability in the Time and Frequency Domains

Time-domain HRV metrics serving as fundamental indicators of cardiac rhythm variability were computed, including the mean (MeanRR), the standard deviation (SDRR) and the root mean square of successive differences (RMSSD) of R-R interval series. Time series were preprocessed using a high-pass autoregressive filter (zero phase, cut-off frequency of 0.0156 Hz) to remove slow baseline drifts. All time series were visually inspected to confirm the stability of their mean and variance within the observation windows. Power spectral density (PSD) was estimated using the non-parametric Blackman–Tukey method[34] with a Hamming window and a spectral bandwidth of 0.04 Hz. Frequency-domain analysis was subsequently performed to characterize HRV spectral components within the very-low-frequency (VLF, ≤ 0.04 Hz), low-frequency (LF, $0.04 - 0.15$ Hz) and high-frequency (HF, $0.15 - 0.4$ Hz) bands during rest. During the exercise phases, the HF band was dynamically adjusted to account for the increase in respiratory rate induced by exertion[12]. Specifically, the dominant respiratory peak was identified within the $0.15 - 1.0$ Hz range and a symmetric ± 0.125 Hz window was identified around this peak to define the exercise-specific HF band[35]. Finally, the power of each band (VLF, LF, HF) was normalized by calculating the ratio of the absolute power in the specific band to the total power of the spectrum.

2.4 Information-theoretic Measures to Characterize Heartbeat Dynamics

We employed information-theoretic measures to investigate the complexity of heartbeat dynamics during graded exercise in HFrEF patients. Specifically, we calculated Shannon entropy (H), conditional entropy (CE) and self-entropy (SE) on the R-R interval time series, to respectively assess the overall signal uncertainty, the residual complexity after accounting for past R-R dynamics, and the predictable information retained by the series[13,16]. The most widely used continuous model-free estimator, i.e., the k-nearest-neighbor (KNN), was used in this work to provide estimates of complexity measures, as well as to capture putative nonlinear behaviors often attributed to physiological mechanisms underlying HRV. The KNN estimator was performed via non-uniform embedding to optimize the description of the system dynamics (the maximum number of scanned neighbors was set to 10); further details about methodology can be found in[16,36].

2.5 Surrogate and Statistical Analysis

To evaluate the statistical significance of the SE measures, as well as to determine the presence of nonlinear dynamics, surrogate data analyses were performed following the framework proposed by Pinto et al.[22]. To test for *self-dependency*, i.e., to assess the statistical significance of the original SE measures, we employed randomly shuffled surrogates with the same mean, variance and probability distribution as the original series but destroying the temporal dependence of the present on the past heartbeats, according to the null hypothesis of fully unpredictable process. On the other hand, to assess the presence of *nonlinear dynamics*, Iterative Amplitude Adjusted Fourier Transform (iAAFT) surrogates were employed. These surrogates retain the linear auto-correlations and amplitude distribution of the original series but destroy its non-linear temporal structure, according to the null hypothesis that the original R-R interval time series comes from a process that exclusively exhibits linear dynamics. Both procedures were repeated $N_s = 1000$ times to derive the corresponding SE surrogate distributions, from which the significance thresholds were derived taking the 95^{th} percentiles. Both null hypotheses were rejected when the original SE values exceeded the thresholds, indicating that the original series is highly self-predictable and/or exhibit evident nonlinearities, respectively.

Non-parametric statistical tests were applied to assess statistically significant differences between physiological indices evaluated in the three phases of the experimental protocol, i.e., Rest, Early and Late conditions, as the distributions of HRV indices across different stages did not always satisfy normality assumptions according to the Anderson–Darling normality test. First, the non-parametric Friedman test was used to assess overall differences across the three conditions, followed by post-hoc pairwise comparisons through the Wilcoxon signed-rank test for paired data. These comparisons were applied to time-domain markers, i.e., MeanRR, SDRR and RMSSD, as well as to frequency bands power (VLF, LF, HF) and to complexity measures of H, CE and SE. To account for multiple comparisons ($n_c = 3$), Bonferroni correction was applied, with statistical significance defined as $p < \alpha/n_c$. For all the analyses, the significance level was set to $\alpha = 0.05$.

2.6 Survival Analysis

Survival analyses were performed to evaluate the association between clinical and functional variables and the risk of cardiovascular death. Time-to-event was defined as the interval from enrollment to the occurrence of cardiovascular death or censoring at the last follow-up. Univariate Cox proportional hazards regression models were fitted separately for each covariate to estimate hazard ratios (HRs) and corresponding 95% confidence intervals (CIs). Statistical significance in univariate analyses was assessed using two-sided Wald tests, with p-values derived from the standard normal distribution. Variables showing an association with the outcome at a predefined threshold ($p < 0.10$) were subsequently included in multivariate Cox proportional hazards models to identify independent prognostic factors. Pearson correlation coefficients were calculated to assess pairwise relationships between variables and to detect potential collinearity before inclusion in multivariable analyses. In multivariate models, the proportional hazards assumption was evaluated using Schoenfeld residuals, and p-values for each covariate were calculated using two-sided Wald tests, with coefficients and standard errors estimated while adjusting for all other variables in

the model. Kaplan–Meier survival curves were generated after stratification of the variable of interest into tertiles (low, medium and high) and differences between groups were assessed using the log-rank test. Survival curves were plotted together with the corresponding numbers at risk.

3 Results

3.1 Variability of Heartbeat Dynamics during Graded Exercise

All assessed HRV metrics show statistically significant differences across exercise stages according to the Friedman test ($p < 0.001$). Figure 1a summarizes the time-domain results. MeanRR significantly decreases with increasing workload across all stages. SDRR shows a significant reduction only during the Late exercise phase, indicating diminished beat-to-beat variability under maximal exertion, while no significant change is observed in the Early exercise phase. RMSSD exhibits a progressive and significant decline across all stages, reflecting a reduction in short-term parasympathetic modulation as physical effort increases.

By looking at the PSD profiles (Figure 2), computed as the median across all subjects, we observe a clear rightward shift of the median HF peak with increasing workload, reflecting the expected rise in respiratory rate. Specifically, the HF band is centered around 0.20–0.45 Hz at the onset of exercise and shifts to approximately 0.30–0.65 Hz during the Late exercise phase. Overall, spectral power decreases progressively across phases, accompanied by this spectral shift, indicating an acceleration of the underlying oscillatory dynamics and a redistribution of autonomic modulation as exercise intensity increases. The absolute power of all considered frequency bands (VLF, LF, HF) uniformly decreases as workload progressed, reflecting the progressive loss of variability. However, when considering the relative power (i.e., the normalized powers), as illustrated in Figure 1b, distinct phase-dependent trends emerge. The normalized power of the VLF band demonstrates a progressive decrease with increasing workload. Conversely, the normalized power of the HF band exhibits the opposite trend, showing a statistically significant increase across the exercise phases. Finally, the normalized power of the LF band remains relatively stable between the Rest and Early exercise phases before showing a statistically significant decrease during the Late exercise stage.

The results of the information-theoretic analyses are shown in Figure 1c. Distinct changes in R-R interval time series complexity are observed across exercise stages. Specifically, H and CE measures increase progressively with workload, indicating greater signal complexity under higher physiological demand. In contrast, SE decreases from Rest to Late exercise, reflecting reduced predictability of heart rate dynamics as exercise intensity increased. Results of surrogate data analysis are shown in Figure 3. The vast majority of subjects shows statistically significant SE values, with 76 out of 77 cases reaching significance in the Rest phase and 100% of cases in both the Early and Late exercise phases. Evidence of nonlinearity is detected in 35 time series during Rest (45.5%), 43 during Early exercise (55.8%) and 70 during Late exercise (90.9%). These results indicate a progressive increase in statistically significant nonlinear HRV components with rising workload, reaching a peak at maximal exercise intensity.

3.2 Comparison between Cardiovascular Death and Surviving Groups

Baseline demographics, clinical characteristics, pharmacological therapy, and peak exercise physiology variables are summarized for the survival and cardiovascular death groups in Table 1, together with the results of the univariate survival analyses. Univariate Cox models show no statistically significant associations between demographic variables and the risk of cardiovascular death. Among clinical measures, lower LVEF and lower SBP are significantly associated with higher mortality risk. No significant associations are observed for prescribed pharmacological therapies. Among exercise tolerance metrics, a higher $\dot{V}E/\dot{V}CO_2$ slope is significantly associated with an increased risk of cardiovascular death, whereas peak oxygen consumption was not significantly associated with outcome.

Regarding HRV, no significant differences are detected between the groups in time-domain parameters across the three exercise stages, nor when considering absolute band powers in the frequency domain, as shown in the Supplementary Figure 1. However, significant group differences emerge when considering the normalized frequency power (Figure 4a) during the Early exercise phase. Specifically, the VLF relative power and the HF relative power showed a discordant pattern between the two groups. VLF relative power is significantly lower in the S group compared to the D group, while the HF relative power is significantly higher in the S group relative to the D group. Similarly, in the information-theoretic domain (Figure 4b), significant group differences also emerge during the Early exercise phase. The CE of the R-R interval time series is lower in the D group compared to survivors, whereas the SE is higher in the D group relative to the surviving group. These specific differences in normalized frequency power and complexity metrics are not observed at Rest or during the Late exercise phase. Across exercise stages, both groups follow the overall pattern described in Figure 1, except for VLF and HF, which do not differ significantly between the Rest and Early stages in the D group.

Where statistically significant differences were detected in HRV metrics, survival analyses were performed. In univariate Cox regression analyses, both CE and SE measured during the early exercise phase demonstrate significant prognostic value for cardiovascular mortality. Higher CE is associated with a markedly reduced risk of cardiovascular death (HR = 0.05, 95% CI

Feature	S=60	D=17	HR	95%CI Lower-Upper	p-values
Demographics					
Age [years]	48.9 (13.3)	52.6 (12.3)	1.02	0.98-1.07	0.307
Sex (F#/M)	17/43	2/15	2.51	0.57-10.98	0.222
Weight [kg]	79.1 (20.6)	77.5 (11.1)	0.99	0.97-1.02	0.643
BMI [kg/m^2]	26.6 (5.0)	28.1 (3.6)	1.07	0.97-1.19	0.190
Clinical Data					
Etiology (IHF#/NIHF)	25/35	7/10	0.89	0.34-2.35	0.812
NYHA	2.4 (0.6)	2.7 (0.8)	2.14	0.92-5.00	0.079
SBP [mmHg]	107.7 (14.4)	99.3 (9.0)	0.94	0.90-0.98	0.007 *
DBP [mmHg]	66.6 (8.7)	62.8 (8.9)	0.95	0.90-1.00	0.072
LVEF [%]	27.9 (6.3)	20.9 (4.3)	0.88	0.81-0.97	0.012 *
ICD	41 (68.3%)	12 (70.6%)	1.12	0.40-3.19	0.825
CRT	7 (11.7%)	5 (29.4%)	2.35	0.83-6.70	0.108
Pharmacological Therapy					
ACE	14 (23.3%)	2 (11.8%)	0.37	0.08-1.64	0.192
ARNI	36 (60.0%)	10 (58.8%)	0.98	0.37-2.57	0.960
β-blockers	57 (95.0%)	16 (94.1%)	1.2	0.16-9.12	0.898
MRA	52 (86.7%)	15 (88.2%)	1.09	0.24-4.80	0.906
Diuretics	44 (73.3%)	13 (76.5%)	1.07	0.35-3.28	0.912
SGLT2	51 (85.0%)	14 (82.4%)	0.80	0.23-2.78	0.724
Peak Exercise Physiology					
$\dot{V}O_2$peak [mL/kg/min]	17.2 (4.6)	18.3 (3.4)	1.02	0.91-1.15	0.730
$\dot{V}E/\dot{V}CO_2$ slope	37.7 (7.6)	44.1 (11.9)	1.06	1.01-1.12	0.018*

Table 1. Comparison of demographics, clinical data, pharmacological therapy and peak exercise physiology measures between surviving (S) and cardiovascular death (D) groups. Continuous variables are reported as mean (standard deviation), while categorical variables are presented as number of patients (percentage within the group). Results of survival analyses are presented, including hazard ratios (HR) with corresponding 95% confidence intervals (CI) lower and upper bounds and p-values, with statistical significance defined as $p < 0.05$ and indicated with *. For categorical variables, reference group is indicated with #.

0.01–0.23, p < 0.001), whereas higher SE shows the opposite pattern, being strongly associated with increased risk (HR = 28.59, 95% CI 4.93–165.79, p < 0.001). In contrast, frequency-domain measures such as normalized VLF power and normalized HF power do not exhibit meaningful prognostic value. Although VLF shows a statistically significant association with mortality (HR = 1.03, 95% CI 1.01–1.06, p = 0.003), the effect size is modest and unlikely to be clinically relevant, while HF does not reach statistical significance (HR = 0.97, 95% CI 0.94–1.01, p = 0.114).

Given the strong inverse correlation between CE and SE during the Early exercise phase (Pearson's $r = -0.969$), only SE is retained for further analyses to avoid collinearity. A multivariate Cox proportional hazards model is constructed by including demographic, clinical, pharmacological and peak exercise physiological variables with $p < 0.1$ in univariate analyses, together with SE measured during the Early exercise phase. No significant violations of the proportional hazards assumption are detected based on Schoenfeld residuals. Results of the multivariate analysis are reported in Table 2. SE measured during the Early exercise phase remains independently associated with cardiovascular mortality after adjustment for significant variables. Higher SE is associated with a significantly increased risk of cardiovascular death (HR = 24.95, 95 % CI 2.00–310.75, p = 0.012). In addition, NYHA functional class emerges as an independent predictor of outcome, whereas systolic and diastolic blood pressure, left ventricular ejection fraction and ventilatory efficiency do not retain statistical significance in the adjusted model. Finally, Kaplan-Meier survival curves stratified by tertiles of SE measured during the early exercise phase (Figure 5) demonstrate a clear stepwise reduction in survival probability with increasing SE values, with patients in the lowest SE tertile exhibiting the most favorable prognosis.

Feature	HR	95%CI Lower-Upper	p-values
NYHA	2.75	1.15-6.61	0.024*
SBP	0.94	0.90-0.98	0.405
DBP	0.95	0.85-1.06	0.353
LVEF	0.97	0.88-1.02	0.151
$\dot{V}E/\dot{V}CO_2$ slope	1.05	0.99-1.12	0.117
SE Early phase	24.95	2.00-310.75	0.012*

Table 2. Results of the multivariate Cox proportional hazards regression analysis, reported as hazard ratios (HR) with corresponding 95% confidence intervals (CI) and p-values. Statistical significance is defined as $p < 0.05$ and is indicated with *.

4 Discussion

The present study provides a comprehensive characterization of HRV dynamics during graded exercise in a cohort of transplant-listed HFrEF patients. To our knowledge, this is the first study to apply information-theoretic complexity measures and surrogate data analysis to describe the workload-dependent evolution of cardiac rhythm in this specific end-stage population. The main findings are threefold: (i) HFrEF patients exhibit a workload-dependent increase in normalized high-frequency power despite a concurrent decline in absolute spectral energy, a dissociation whose mechanistic underpinnings are discussed below; (ii) exercise unmasks significant nonlinear dynamics, with a progressive increase in signal complexity (CE) and a loss of self-predictability (SE) as workload increases; and (iii) specific metrics of autonomic complexity and spectral power measured during the early phase of exercise exhibit statistically significant differences between survivors and those who subsequently succumb to cardiovascular death, suggesting the potential prognostic value of physiological responsiveness to mild stress.

4.1 Modulation of Heart Rate Variability during Graded Exercise

Traditional HRV analysis confirms the expected physiological response to exercise. Time-domain metrics (MeanRR, RMSSD) decrease progressively with increasing workload, reflecting the net effect of sympathetic activation and vagal withdrawal required to increase cardiac output[5]. However, global variability (SDRR) declines significantly only at maximal exertion. This delayed reduction in variability is informative given that MeanRR and RMSSD, which capture mean cycle length and short-term beat-to-beat variability respectively, are sensitive to the immediate autonomic shifts accompanying each incremental workload. SDRR, by contrast, integrates variability across all frequencies and longer time scales, and may therefore require a more sustained or pronounced autonomic drive before exhibiting statistically significant changes. This pattern is consistent with the blunted autonomic responsiveness characteristic of chronotropic incompetence[37]. A plausible contributing mechanism may involve the intrinsic down regulation of β-adrenergic receptors typical of HFrEF, compounded by the competitive antagonism of high-dose β-blocker therapy (94.81% prevalence in this cohort). This pharmacological blockade could shield the sinus node from early sympathetic inputs, preventing the rapid heart rate acceleration and variability reduction typically seen at the onset of exercise. Under this hypothesis, significant reductions in SDRR would occur only at maximal physiological drive, when the overall autonomic and neurohormonal demand becomes sufficient to produce measurable changes in global variability[37]. However, as circulating catecholamine levels and direct autonomic indices were not measured in this study, this interpretation remains speculative and should be regarded as a hypothesis requiring prospective validation.

Regarding spectral analysis, absolute power across all frequency bands decreased progressively with rising workload, consistent with the well-established global reduction in total HRV power during exercise as autonomic resources become exhausted[12,38]. In contrast, the normalized spectral components exhibited a distinct pattern: HF normalized power increases significantly at higher intensities, even though its absolute magnitude continued to fall. This pattern has been reported previously and reflects the mathematical effect of normalization under conditions of reduced total power rather than true preservation of vagal modulation[12].

At higher workloads, when neural autonomic regulation becomes saturated, the sinoatrial node remains sensitive to mechanical stretch arising from increased tidal volume and elevated respiratory frequency. Cardiac mechano-electric coupling provides a well-documented mechanism through which such respiratory-induced stretch can modulate pacemaker activity independently of vagal input[39]. Therefore, the apparent dominance of the HF component at peak exercise is more plausibly explained by non-neural, respiration-driven modulation rather than sustained vagal tone. This interpretation is further supported by the rightward shift of the HF spectral peak, which closely tracked the increasing respiratory rate, an expected phenomenon given that the HF band is defined by and anchored to the respiratory frequency[12].

4.2 The Nonlinearity Paradox and Loss of Homeostatic Control

Information-theoretic analysis provides complementary insights. Graded exercise produces a progressive increase in signal complexity (H and CE) accompanied by a reduction in self-predictability (SE). Surrogate data analysis further confirmed a significant development of nonlinear dynamics[17,22]. Notably, SDRR decreased significantly only at maximal exertion, whereas entropy measures changed progressively from the early stages of exercise, suggesting that complexity and predictability of heartbeat dynamics may serve as more sensitive markers of autonomic dysregulation than variance-based indices alone. Shannon entropy primarily reflects overall signal uncertainty, closely related to variance, whereas nonlinear entropy-based metrics detect departures from Gaussian and linearly correlated dynamics in HRV time series, thereby revealing alterations in the underlying regulatory structure that conventional measures may not capture[20,40].

Interpreting these findings requires comparison with known exercise-related HRV dynamics in healthy individuals, where increasing workload typically reduces nonlinearity due to sympathetic dominance and sinus node regularization[41,42]. However, DFA-based analyses in healthy athletes demonstrate a more nuanced, biphasic pattern: the short-term fractal scaling exponent initially increases from rest to low exercise intensities, then undergoes a near-linear decline from moderate workloads to exhaustion, reflecting a progressive breakdown of autonomous heart rate regulation and a shift toward non-autonomic control mechanisms at high intensities[9]. This indicates that even in healthy individuals, high-intensity exercise can induce a loss of long-range correlations and a qualitative change in self-organized cardiac regulation. The patterns observed in the present cohort may therefore share mechanistic features with this physiological response to maximal loading. However, in heart failure, such regulatory breakdown is likely exacerbated and occurs at substantially lower workloads, due to impaired chronotropic reserve, reduced autonomic adaptability and the superimposition of pathological oscillatory mechanisms.

From an interpretative standpoint, the progressive rise in nonlinear complexity across exercise stages suggests that autonomic regulation under stress transitions toward less tightly and more weakly correlated regulatory patterns, rather than converging on uniform sympathetic control. This is consistent with the *loss of complexity* hypothesis[43,44]. While healthy systems exhibit structured, adaptive complexity, regulatory systems under pathological stress may exhibit a relatively more noise-like and less correlated behavior, registering as high entropy but reflecting a breakdown of homeostatic control rather than healthy adaptability. In the context of heart failure, this may manifest as destabilized regulatory dynamics, irregular interactions among neural, mechanical, and humoral oscillators, or compensatory feedback mechanisms when chronotropic reserve is exhausted. Nonlinear HRV complexity has accordingly been shown to be more sensitive than conventional HRV metrics in detecting altered autonomic and cardiovascular control[7,45,46], and prior studies have linked nonlinear HRV indices to worsened prognosis in heart failure, including mortality and heart transplantation[47–49]. These findings represent associations; altered entropy should be interpreted as a marker of disease severity or reduced autonomic adaptability, not as a mechanistic driver of adverse events.

Overall, the increase in nonlinear complexity with workload in this cohort can be interpreted as the convergence of compensatory destabilization, progressive loss of autonomic reserve, and activation of pathological oscillatory mechanisms, including baroreflex dysfunction, arrhythmogenic substrate, or neurohormonal surges. These dynamics evolve progressively under exercise stress, providing insight into residual autonomic regulatory capacity that may not be captured by linear HRV measures alone.

4.3 Early Exercise HRV Highlight Differences between Groups

The Early stage of exercise reveals significant group differences in the normalized spectral components of HRV, though their prognostic capacity appeared distinct from their statistical separation. Specifically, the D group exhibits higher VLF relative power and lower HF relative power than survivors. This divergent pattern may reflect two complementary aspects of autonomic dysregulation. Reduced HF power during mild exercise suggests blunted respiratory–vagal modulation, consistent with impaired parasympathetic responsiveness and reduced cardiopulmonary coupling[50]. Conversely, elevated VLF power, despite declining absolute spectral energy, may indicate an abnormal amplification of slower oscillatory components linked to impaired baroreflex sensitivity, neurohormonal activation, peripheral chemoreflex drive or increased long-term regulatory instability. In heart failure, excessive VLF activity has been associated with heightened sympathetic tone, renin–angiotensin–aldosterone system activation and poorer prognosis[51–53]. However, when subjected to survival analysis, these frequency-domain measures do not exhibit meaningful prognostic value, indicating that linear spectral imbalance alone may lack the robustness required for individual risk stratification in this advanced heart failure cohort. Nonetheless, interpretation of VLF in short-term HRV should be approached with caution due to its limited reliability[6].

In contrast, entropy-based metrics not only distinguished patients who later experienced adverse outcomes from survivors during early exercise, but also showed a significant association with outcome in survival analyses. Complexity was lower and self-predictability higher in patients who deteriorated, suggesting that altered complexity under moderate physiological stress may serve as an early marker of reduced adaptability. This aligns with the concept that stress testing can reveal latent autonomic vulnerabilities[54] and may point toward a potential prognostic role of nonlinear HRV measures beyond traditional clinical variables[48]. Importantly, several established prognostic markers in heart failure were significantly associated with outcome

in univariate analyses. Higher SBP likely reflects a better preserved haemodynamic reserve in the survival group, whereas a higher $\dot{V}E/\dot{V}CO_2$ slope indicates greater ventilatory inefficiency in the cardiovascular death group. In addition, LVEF was lower in the D group, consistent with more severe cardiac dysfunction. Despite the prognostic relevance of these established markers, SE measured at submaximal workload showed a stronger association with adverse outcomes in the multivariate model of this cohort. It is important to note that, given the advanced end-stage nature of this heart failure cohort, all patients exhibited universally impaired maximal exercise capacity, resulting in no significant differences in maximal exercise metrics between the groups. Furthermore, given the limited number of adverse events, multivariate analyses should be interpreted cautiously and considered exploratory.

The convergence of higher Early phase VLF, lower HF, reduced CE and elevated SE in the D group therefore suggests that patients who later deteriorated display an early inability to reorganize autonomic modulation during physiological challenge. Rather than demonstrating the expected transition to efficient vagally modulated respiratory entrainment, these patients show a shift toward slower, more unstable oscillations and more predictable heartbeat dynamics, hallmarks of reduced autonomic adaptability[47]. Thus, submaximal exercise appears to expose impairments in short-term autonomic flexibility that are not evident at rest or during maximal stress. Spectral and entropy-based metrics capture complementary signatures of this maladaptive response. Importantly, early exercise represents a clinically feasible and low-risk phase that can be assessed even in patients unable to sustain maximal workloads[55].

We acknowledge that the electrical substrate necessitating device therapy, such as left bundle branch block or intraventricular conduction delays, may inherently alter beat-to-beat dynamics independent of autonomic modulation[56]. Furthermore, CRT itself has been shown to acutely modify autonomic balance and HRV parameters[57]. However, given that device prevalence was comparable between survivors and non-survivors in our study, it is unlikely that device presence alone drove the prognostic divergence observed in the entropy metrics. Instead, nonlinear alterations likely reflect the composite effect of the underlying cardiomyopathy and the exhausted autonomic reserve characteristic of this terminal population.

4.4 Limitations and Future Studies

The findings of this study must be interpreted in light of several limitations. Firstly, the relatively small sample size, particularly for prognostic analyses, alongside the focus on a highly selected population of patients referred for advanced heart failure assessment, may constrain the generalizability of our conclusions to broader cardiovascular cohorts. Secondly, the influence of concurrent pharmacologic and device therapies on HRV metrics presents a potential source of confounding factors that could have modulated the observed physiological responses. Finally, from a methodological standpoint, the reliance on short-term exercise recordings, while offering high temporal resolution, renders the measurements potentially sensitive to non-stationary effects. Furthermore, the specificity of the findings may be dependent upon the specific entropy measures and signal preprocessing methods employed in the HRV analysis. Future investigations are warranted to address these limitations and advance our understanding. Subsequent studies should adopt a more holistic physiological viewpoint by incorporating simultaneous recordings of other key physiological signals, such as respiratory and metabolic parameters, to provide a richer context for interpreting cardiac autonomic function. It is worth highlighting that, in this study, ventricular ectopic beats were corrected; future research could instead retain these events and combine HRV metrics with ectopy-derived indices, such as heart rate turbulence, to provide complementary prognostic information in HFrEF. Finally, improving the external validity of the research will necessitate the inclusion of appropriate control groups, specifically a healthy control group or subjects with moderated cardiovascular impairment, to better benchmark the autonomic profile of the highly-selected patient population.

5 Conclusions

In this study, graded exercise induced marked alterations in both linear and nonlinear heart rate variability dynamics in HFrEF patients. Conventional time- and frequency-domain indices exhibited the expected attenuation associated with exercise-induced vagal withdrawal. In contrast, information-theoretic analyses revealed a progressive increase in R–R interval time series complexity and a growing contribution of nonlinear dynamics with increasing workload. This pattern departs from the sympathetic-driven regularization typically observed in healthy individuals and instead points toward impaired autonomic regulation under physiological stress in HFrEF. Notably, entropy-based measures, specifically conditional entropy and self-entropy, obtained during the early phase of exercise distinguished patients who subsequently experienced adverse cardiovascular outcomes from those who survived and showed an association with outcome in this cohort. These findings suggest that assessing cardiac rhythm predictability during submaximal exercise may provide additional insight into autonomic dynamics that are not apparent at rest and may not be fully captured by conventional HRV metrics. Nonetheless, these results should be interpreted as a preliminary investigation, given the limited number of outcome events and the absence of external validation. Further studies in larger and independent cohorts will be necessary to confirm the potential role of information-theoretic HRV measures during exercise in characterizing autonomic dysfunction and in future risk stratification research in advanced heart failure.

Data Availability

The datasets generated and/or analysed during the current study are available from the corresponding author on reasonable request. The software relevant to the estimation of entropy-based measures is part of the ITS toolbox, which is freely available for download at www.lucafaes.net/its.html.

References

1. Groenewegen, A., Rutten, F. H., Mosterd, A. & Hoes, A. W. Epidemiology of heart failure. *Eur. J. Hear. Fail.* **22**, 1342–1356, DOI: https://doi.org/10.1002/ejhf.1858 (2020).
2. Savarese, G. *et al.* Global burden of heart failure: a comprehensive and updated review of epidemiology. *Cardiovasc. Res.* **118**, 3272–3287, DOI: https://doi.org/10.1093/cvr/cvac013 (2022).
3. Gentile, F. *et al.* Treating heart failure by targeting the vagus nerve. *Hear. Fail. Rev.* **29**, 1201–1215, DOI: https://doi.org/10.1007/s10741-024-10430-w (2024).
4. Murphy, S. P., Ibrahim, N. E. & Januzzi, J. L. Heart failure with reduced ejection fraction: A review. *JAMA* **324**, 2107–2108, DOI: https://doi.org/10.1001/jama.2020.21736 (2020).
5. Task Force of the European Society of Cardiology and the North American Society of Pacing and Electrophysiology. Heart rate variability: standards of measurement, physiological interpretation, and clinical use. *Circulation* **93**, 1043–1065, DOI: https://doi.org/10.1161/01.CIR.93.5.1043 (1996).
6. Shaffer, F. & Ginsberg, J. P. An overview of heart rate variability metrics and norms. *Front. Public Heal.* **5**, DOI: https://doi.org/10.3389/fpubh.2017.00258 (2017).
7. Tsai, C. H. *et al.* Usefulness of heart rhythm complexity in heart failure detection and diagnosis. *Sci. Reports* **10**, DOI: https://doi.org/10.1038/s41598-020-71909-8 (2020).
8. Binder, T. *et al.* Prognostic value of heart rate variability in patients awaiting cardiac transplantation. *Pacing Clin. Electrophysiol.* **15**, 2215–2220, DOI: https://doi.org/10.1111/j.1540-8159.1992.tb03050.x (1992).
9. Gronwald, T., Hoos, O., Ludyga, S. & Hottenrott, K. Non-linear dynamics of heart rate variability during incremental cycling exercise. *Res. Sports Medicine* **27**, 88–98, DOI: https://doi.org/10.1080/15438627.2018.1502182 (2019). PMID: 30040499.
10. Goldberger, A. L. *et al.* Fractal dynamics in physiology: alterations with disease and aging. *Proc. Natl. Acad. Sci.* **99**, 2466–2472, DOI: https://doi.org/10.1073/pnas.012579499 (2002).
11. Paolillo, S. *et al.* Heart rate during exercise: mechanisms, behavior, and therapeutic and prognostic implications in heart failure patients with reduced ejection fraction. *Hear. Fail. Rev.* **23**, 537–545, DOI: https://doi.org/10.1007/s10741-018-9712-1 (2018).
12. Michael, S., Graham, K. S. & Davis, G. M. Cardiac autonomic responses during exercise and post-exercise recovery using heart rate variability and systolic time intervals — a review. *Front. Physiol.* **8**, 301, DOI: https://doi.org/10.3389/fphys.2017.00301 (2017).
13. Azami, H., Faes, L., Escudero, J., Humeau-Heurtier, A. & Silva, L. E. *Entropy Analysis of Univariate Biomedical Signals: Review and Comparison of Methods*, chap. 9, 233–286 (2023).
14. Javorka, M. *et al.* Towards understanding the complexity of cardiovascular oscillations: Insights from information theory. *Comput. Biol. Medicine* **98**, 48–57, DOI: https://doi.org/10.1016/j.compbiomed.2018.05.007 (2018).
15. Pernice, R. *et al.* Comparison of short-term heart rate variability indexes evaluated through electrocardiographic and continuous blood pressure monitoring. *Med. & Biol. Eng. & Comput.* **57**, 1247–1263, DOI: https://doi.org/10.1007/s11517-019-01957-4 (2019).
16. Barà, C. *et al.* Comparison of entropy rate measures for the evaluation of time series complexity: Simulations and applications. *Biocybern. Biomed. Eng.* **44**, 380–392, DOI: https://doi.org/10.1016/j.bbe.2024.04.004 (2024).
17. Faes, L. *et al.* Comparison of methods for the assessment of nonlinearity in short-term heart rate variability under different physiopathological states. *Chaos: An Interdiscip. J. Nonlinear Sci.* **29**, 123114, DOI: https://doi.org/10.1063/1.5115506 (2019).
18. Mayer, C. C. *et al.* Selection of entropy-measure parameters for knowledge discovery in heart rate variability data. *BMC Bioinforma.* **15**, S2, DOI: https://doi.org/10.1186/1471-2105-15-S6-S2 (2014).

19. Huikuri, H. V., Mäkikallio, T. H. & Perkiömäki, J. Measurement of heart rate variability by methods based on nonlinear dynamics. *J. Electrocardiol.* **36**, 95–99, DOI: https://doi.org/10.1016/j.jelectrocard.2003.09.021 (2003).

20. Chen, C. *et al.* Complexity change in cardiovascular disease. *Int. J. Biol. Sci.* **13**, 1320, DOI: https://doi.org/10.7150/ijbs.19462 (2017).

21. Xiong, W., Faes, L. & Ivanov, P. C. Entropy measures, entropy estimators, and their performance in quantifying complex dynamics: Effects of artifacts, nonstationarity, and long-range correlations. *Phys. Rev. E* **95**, 062114, DOI: https://doi.org/10.1103/PhysRevE.95.062114 (2017).

22. Pinto, H. *et al.* Testing dynamic correlations and nonlinearity in bivariate time series through information measures and surrogate data analysis. *Front. Netw. Physiol.* **Volume 4 - 2024**, DOI: https://doi.org/10.3389/fnetp.2024.1385421 (2024).

23. Nagai, M. *et al.* Heart rate variability and heart failure with reduced ejection fraction: A systematic review of literature. *Curr. Cardiol. Rev.* **21**, 78–87, DOI: https://doi.org/10.2174/011573403X327105241021180916 (2025).

24. Sempere-Ruiz, N. *et al.* Detection of exercise intensity thresholds in patients with chronic heart failure based on correlation properties of heart rate variability. *Eur. J. Appl. Physiol.* **125**, 3475–3484, DOI: 10.1007/s00421-025-05860-9 (2025).

25. Gronwald, T., Rogers, B. & Hoos, O. Fractal correlation properties of heart rate variability: A new biomarker for intensity distribution in endurance exercise and training prescription? *Front. Physiol.* **Volume 11 - 2020**, DOI: 10.3389/fphys.2020.550572 (2020).

26. Myers, J. & Bellin, D. Ramp exercise protocols for clinical and cardiopulmonary exercise testing. *Sports Medicine* **30**, 23–29, DOI: https://doi.org/10.2165/00007256-200030010-00003 (2000).

27. Juarez, M., Castillo-Rodriguez, C., Soliman, D., Del Rio-Pertuz, G. & Nugent, K. Cardiopulmonary exercise testing in heart failure. *J. Cardiovasc. Dev. Dis.* **11**, DOI: 10.3390/jcdd11030070 (2024).

28. Faes, L., Porta, A. & Nollo, G. Information decomposition in bivariate systems: Theory and application to cardiorespiratory dynamics. *Entropy* **17**, 277–303, DOI: 10.3390/e17010277 (2015).

29. Pan, J. & Tompkins, W. J. A real-time qrs detection algorithm. *IEEE Transactions on Biomed. Eng.* **BME-32**, 230–236, DOI: https://doi.org/10.1109/TBME.1985.325532 (1985).

30. Volpes, G. *et al.* Feasibility of ultra-short-term analysis of heart rate and systolic arterial pressure variability at rest and during stress via time-domain and entropy-based measures. *Sensors* **22**, DOI: https://doi.org/10.3390/s22239149 (2022).

31. Shaffer, F., Meehan, Z. M. & Zerr, C. L. A critical review of ultra-short-term heart rate variability norms research. *Front. Neurosci.* **14**, DOI: https://doi.org/10.3389/fnins.2020.594880 (2020).

32. Castaldo, R., Montesinos, L., Melillo, P., James, C. & Pecchia, L. Ultra-short term hrv features as surrogates of short term hrv: a case study on mental stress detection in real life. *BMC Med. Informatics Decis. Mak.* **19**, 12, DOI: https://doi.org/10.1186/s12911-019-0742-y (2019).

33. Castelbuono, S., Barà, C., Pernice, R., Faes, L. & Bellavia, D. Ultra-short-term heart rate variability of home-monitored heart failure patients: a case study. In *2024 13th Conference of the European Study Group on Cardiovascular Oscillations (ESGCO)*, 1–2, DOI: https://doi.org/10.1109/ESGCO63003.2024.10766984 (2024).

34. Blackman, R. B. & Tukey, J. W. *The Measurement of Power Spectra* (Dover Publications, New York, 1958).

35. Orini, M. *et al.* A method for continuously assessing the autonomic response to music-induced emotions through hrv analysis. *Med. & Biol. Eng. & Comput.* **48**, 423–433, DOI: 10.1007/s11517-010-0592-3 (2010).

36. Faes, L., Kugiumtzis, D., Nollo, G., Jurysta, F. & Marinazzo, D. Estimating the decomposition of predictive information in multivariate systems. *Phys. Rev. E* **91**, 032904, DOI: https://doi.org/10.1103/PhysRevE.91.032904 (2015).

37. Brubaker, P. H. & Kitzman, D. W. Chronotropic incompetence: causes, consequences, and management. *Circulation* **123**, 1010–1020, DOI: https://doi.org/10.1161/CIRCULATIONAHA.110.949619 (2011).

38. Perini, R. & Veicsteinas, A. Heart rate variability and autonomic activity at rest and during exercise in various physiological conditions. *Eur. J. Appl. Physiol.* **90**, 317–325, DOI: https://doi.org/10.1007/s00421-003-0953-9 (2003).

39. Quinn, T. A. & Kohl, P. Cardiac mechano-electric coupling: Acute effects of mechanical stimulation on heart rate and rhythm. *Physiol. Rev.* **101**, 37–92, DOI: https://doi.org/10.1152/physrev.00036.2019 (2021).

40. Kanters, J., Højgaard, M., Agner, E. & Holstein-Rathlou, N. Short- and long-term variations in non-linear dynamics of heart rate variability. *Cardiovasc. Res.* **31**, 400–409, DOI: https://doi.org/10.1016/s0008-6363(95)00085-2 (1996).

41. Solís-Montufar, E. E., Gálvez-Coyt, G. & Muñoz-Diosdado, A. Entropy analysis of rr-time series from stress tests. *Front. Physiol.* **11**, 981, DOI: https://doi.org/10.3389/fphys.2020.00981 (2020).

42. Weippert, M., Behrens, M., Rieger, A. & Behrens, K. Sample entropy and traditional measures of heart rate dynamics reveal different modes of cardiovascular control during low intensity exercise. *Entropy* **16**, 5698–5711, DOI: https://doi.org/10.3390/e16115698 (2014).

43. Costa, M., Goldberger, A. L. & Peng, C.-K. Multiscale entropy analysis of complex physiologic time series. *Phys. Rev. Lett.* **89**, 068102, DOI: https://doi.org/10.1103/PhysRevLett.89.068102 (2002).

44. Vaillancourt, D. E. & Newell, K. M. Changing complexity in human behavior and physiology through aging and disease. *Neurobiol. Aging* **23**, 1–11, DOI: https://doi.org/10.1016/s0197-4580(01)00247-0 (2002).

45. Castillo-Aguilar, M., Mabe-Castro, D., Medina, D. & Núñez-Espinosa, C. Enhancing cardiovascular monitoring: a non-linear model for characterizing rr interval fluctuations in exercise and recovery. *Sci. Reports* **15**, 8628, DOI: https://doi.org/10.1038/s41598-025-93654-6 (2025).

46. Henriques, T. *et al.* Nonlinear methods most applied to heart-rate time series: A review. *Entropy* **22**, DOI: https://doi.org/10.3390/e22030309 (2020).

47. Ho, Y.-L., Lin, C., Lin, Y.-H. & Lo, M.-T. The prognostic value of non-linear analysis of heart rate variability in patients with congestive heart failure—a pilot study of multiscale entropy. *PLOS ONE* **6**, 1–6, DOI: https://doi.org/10.1371/journal.pone.0018699 (2011).

48. Zeid, S. *et al.* Heart rate variability: reference values and role for clinical profile and mortality in individuals with heart failure. *Clin. Res. Cardiol.* **113**, 1317–1330, DOI: https://doi.org/10.1007/s00392-023-02248-7 (2024).

49. Maestri, R. *et al.* Clinical correlates of non-linear indices of heart rate variability in chronic heart failure patients. *Biomed. Eng. / Biomedizinische Tech.* **51**, 220–223, DOI: https://doi.org/10.1515/BMT.2006.041 (2006).

50. Montano, N. *et al.* Power spectrum analysis of heart rate variability to assess the changes in sympathovagal balance during graded orthostatic tilt. *Circulation* **90**, 1826–1831, DOI: https://doi.org/10.1161/01.cir.90.4.1826 (1994).

51. Bigger, J. T., Fleiss, J. L., Rolnitzky, L. M. & Steinman, R. C. Frequency domain measures of heart period variability and mortality after myocardial infarction. *Circulation* **85**, 164–171, DOI: https://doi.org/10.1161/01.CIR.85.1.164 (1992).

52. La Rovere, M. T. *et al.* Prognostic implications of baroreflex sensitivity in heart failure patients in the beta-blocking era. *J. Am. Coll. Cardiol.* **53**, 193–199, DOI: https://doi.org/10.1016/j.jacc.2008.09.034 (2009).

53. Hadase, M. *et al.* Very low frequency power of heart rate variability is a powerful predictor of clinical prognosis in patients with congestive heart failure. *Circ. J.* **68**, 343–347, DOI: https://doi.org/10.1253/circj.68.343 (2004).

54. Dewey, F. E. *et al.* Novel predictor of prognosis from exercise stress testing: Heart rate variability response to the exercise treadmill test. *Am. Hear. J.* **153**, 281–288, DOI: https://doi.org/10.1016/j.ahj.2006.11.001 (2007).

55. Reed, J. L. *et al.* Submaximal exercise testing in cardiovascular rehabilitation settings (best study). *Front. Physiol.* **Volume 10 - 2019**, DOI: 10.3389/fphys.2019.01517 (2020).

56. Alonso, C. *et al.* Effects of cardiac resynchronization therapy on heart rate variability in patients with chronic systolic heart failure and intraventricular conduction delay. *The Am. J. Cardiol.* **91**, 1144–1147, DOI: https://doi.org/10.1016/S0002-9149(03)00171-1 (2003).

57. Braunschweig, F. *et al.* Monitoring of physical activity and heart rate variability in patients with chronic heart failure using cardiac resynchronization devices. *The Am. J. Cardiol.* **95**, 1104–1107, DOI: https://doi.org/10.1016/j.amjcard.2004.12.069 (2005).

Funding

This research was funded by the Italian Ministry of Health, Ricerca Corrente.

Author Contributions Statement

S.C.: study conception and design, analysis and interpretation of data, drafting of manuscript, critical revision. D.B.: study conception and design, analysis and interpretation of data, drafting of manuscript, critical revision. L.S.: analysis and interpretation of data, drafting of manuscript, critical revision. Y.A.: analysis and interpretation of data, drafting of manuscript, critical revision. R.P. analysis and interpretation of data, drafting of manuscript, critical revision. E.L.F.: data collection, critical revision. V.N. data collection, critical revision. P.M.: data collection, critical revision. F.B.: data collection. V.A.: funding acquisition, project administration. M.C.: funding acquisition, critical revision. L.F. study conception and design, analysis and interpretation of data, drafting of manuscript, critical revision, supervision.

Abbreviations

ACE, angiotensin-converting enzyme; ARNI, angiotensin receptor–neprilysin inhibitor; BMI, body mass index; CE, conditional entropy; CRT, cardiac resynchronization therapy; DBP, diastolic blood pressure; ECG, electrocardiogram; HF, high frequency; HFrEF, heart failure with reduced ejection fraction; HR, hazard ratio; HRV, heart rate variability; ICD, implantable cardioverter-defibrillator; IQR, interquartile range; IHF, ischemic heart failure; KNN, k-nearest neighbors; LF, low frequency; LVAD, left ventricular assist device; LVEF, left ventricular ejection fraction; MeanRR, mean R–R interval; MRA, mineralocorticoid receptor antagonist; NIHF, non-ischemic heart failure; NYHA, New York Heart Association; PSD, power spectral density; RMSSD, root mean square of successive differences; SBP, systolic blood pressure; SDRR, standard deviation of R–R intervals; SE, self-entropy; SGLT2, sodium–glucose cotransporter 2; VLF, very low frequency; $\dot{V}E/\dot{V}CO_2$, ventilatory efficiency; $\dot{V}O_2$peak, peak oxygen consumption.

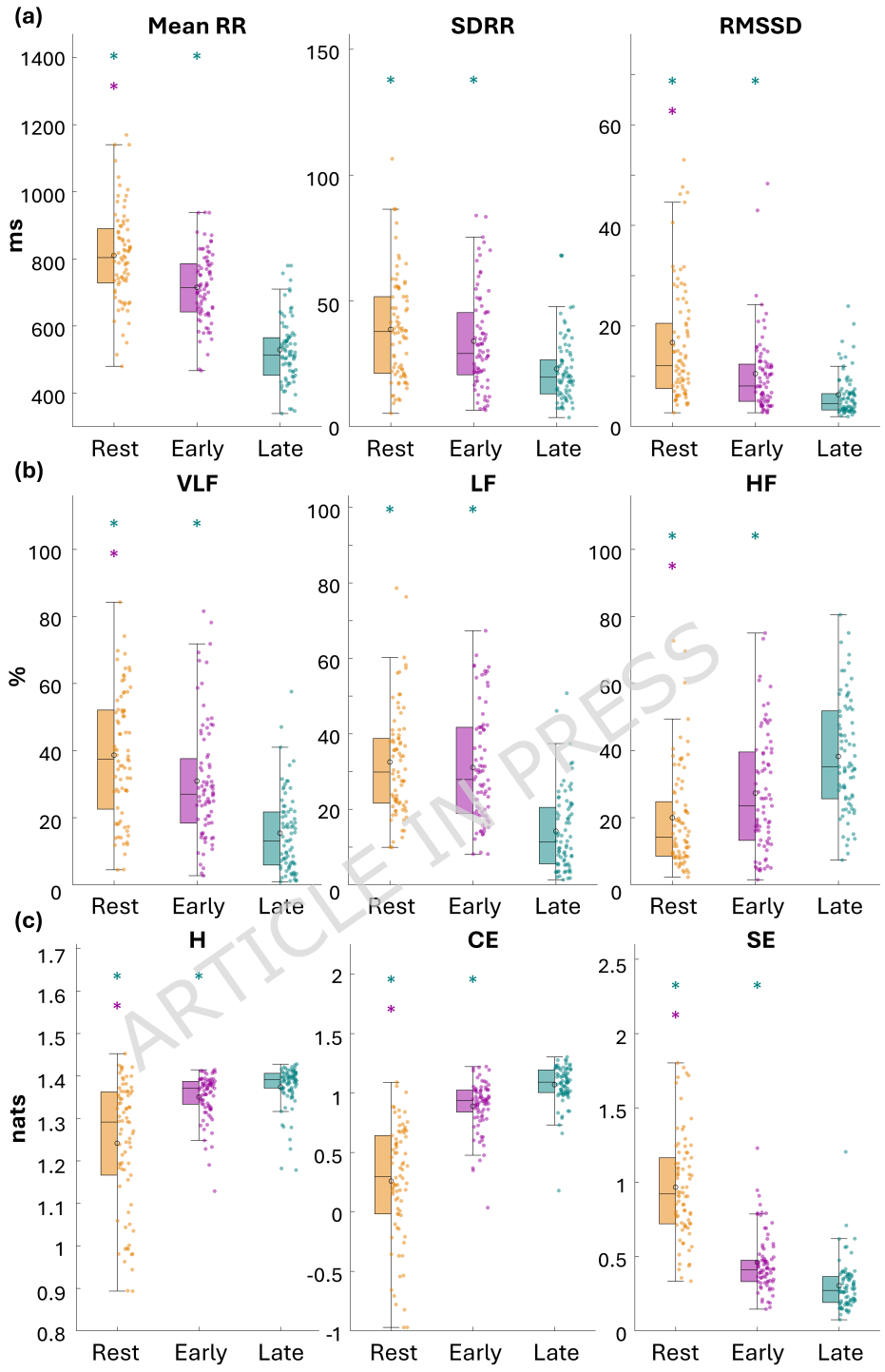

Figure 1. Distribution of HRV metrics. (a) Time-domain HRV [ms]. Boxplots depict MeanRR (left), SDRR (center) and RMSSD (right). (b) Frequency-domain HRV [%]. Boxplots depict normalized very low frequency (VLF, left), low frequency (LF, center) and high frequency (HF, right) power. (c) Information-theoretic domain HRV [nats]. Boxplots depict entropy (H, left), conditional entropy (CE, center) and self-entropy (SE, right). The boxplots illustrate the distribution of the data: the central line within the box represents the median (50^{th} percentile); the box edges denote the first quartile (Q_1, 25^{th} percentile) and the third quartile (Q_3, 75^{th} percentile), with the box length representing the Interquartile Range (IQR: $Q_3 - Q_1$). The whiskers extend to the most extreme data points that are no more than 1.5 times the IQR away from the box. Wilcoxon signed-rank test for paired data: purple, Rest vs. Early; teal, Rest or Early vs. Late, (*) $p < 0.05/3$.

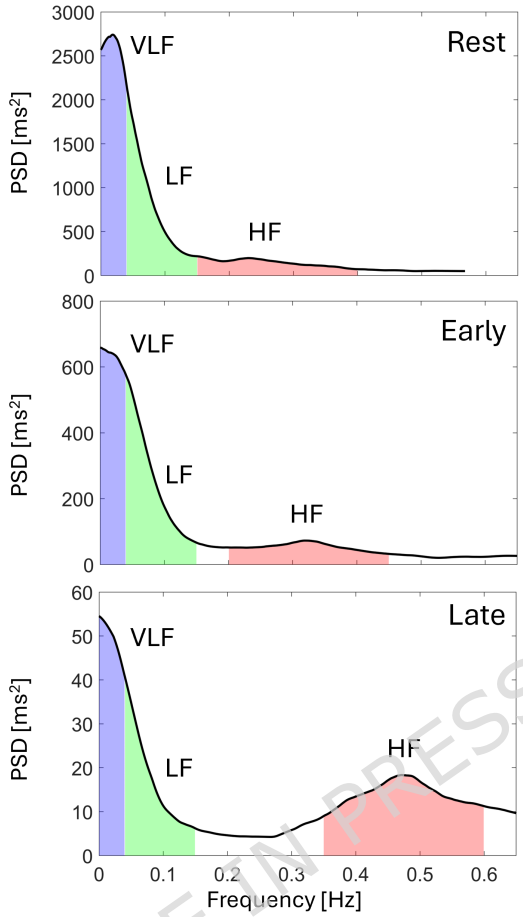

Figure 2. Frequency-domain HRV results. Power Spectral Density (PSD) profiles computed as the median across all subjects (VLF, blue; LF, green; HF, red) across the three exercise phases.

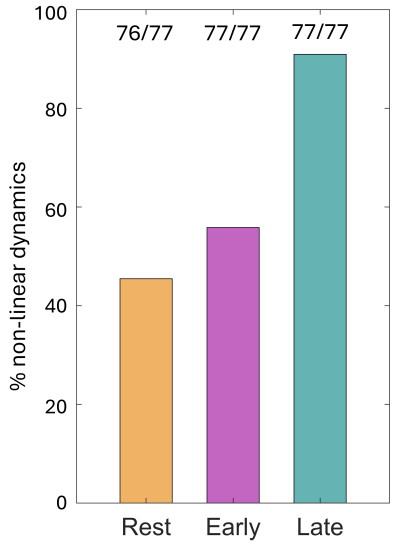

Figure 3. Surrogate data analysis results for Self-Entropy (SE) statistical assessment across the three exercise stages. Bars represent the percentage of RR time series exhibiting statistically significant nonlinear dynamics. Numbers above each bar report the count of time series showing a significant SE value.

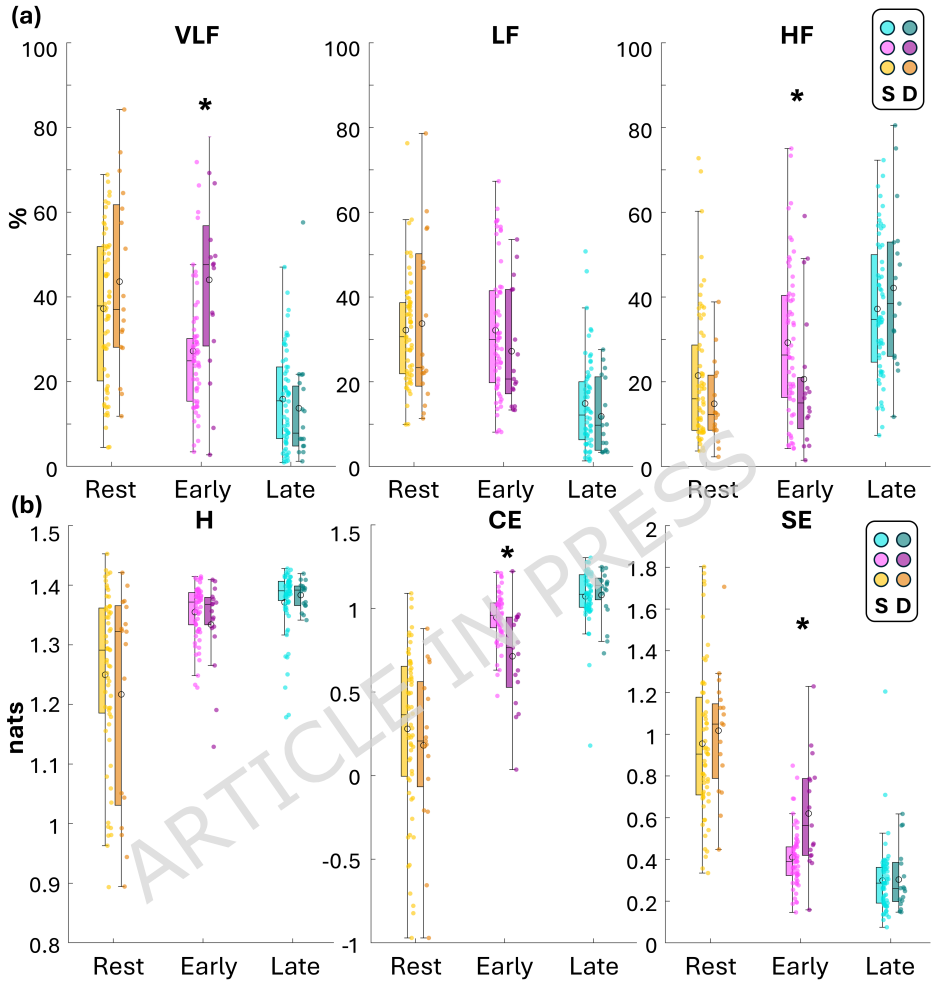

Figure 4. Distribution of HRV metrics across groups. (a) Frequency-domain HRV [%]. Boxplots depict normalized very low frequency (VLF, left), low frequency (LF, center) and high frequency (HF, right) power. (b) Information-theoretic domain HRV [nats]. Boxplots depict entropy (H, left), conditional entropy (CE, center) and self-entropy (SE, right). The boxplots illustrate the distribution of the data: the central line within the box represents the median (50^{th} percentile); the box edges denote the first quartile (Q_1, 25^{th} percentile) and the third quartile (Q_3, 75^{th} percentile), with the box length representing the Interquartile Range (IQR: $Q_3 - Q_1$). The whiskers extend to the most extreme data points that are no more than 1.5 times the IQR away from the box. Clearer colors represent survivors (S, left distributions; n=60) and darker colors represent patients who experienced cardiovascular death (D, right distributions; n=17). Wilcoxon rank-sum test for unpaired data: (*) $p < 0.05/3$.

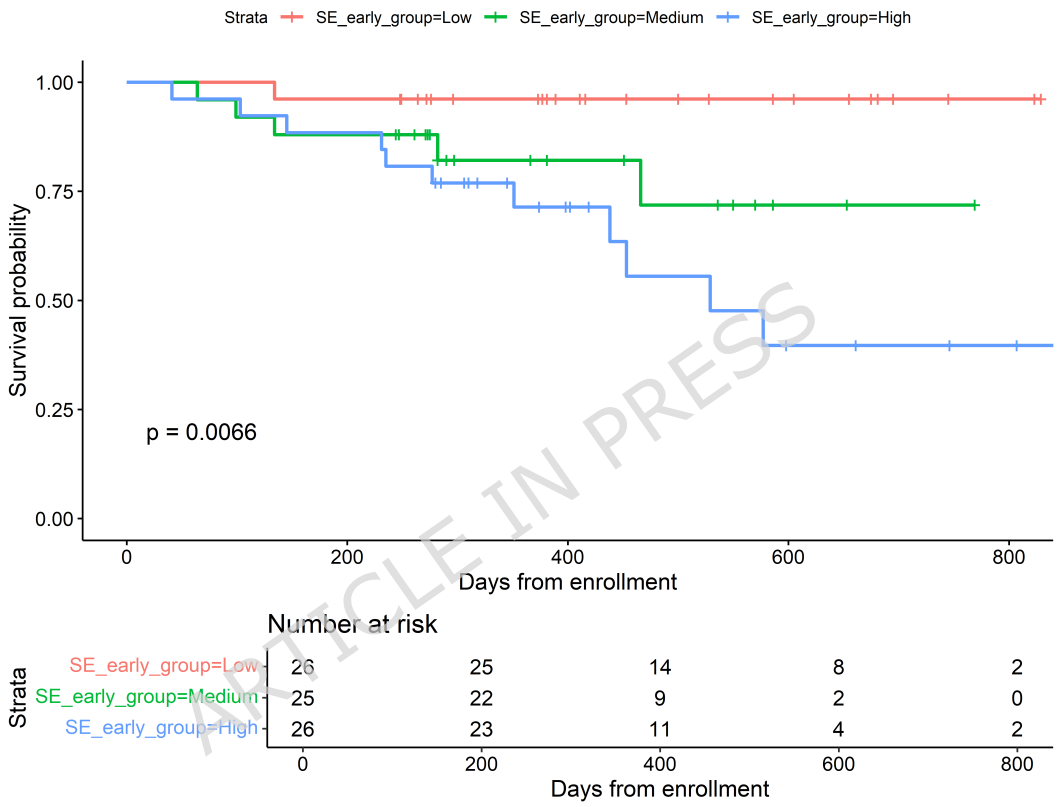

Figure 5. Kaplan–Meier curves depicting cardiovascular survival stratified by tertiles of self-entropy (SE) values measured during the early exercise phase. Subjects were divided into three groups based on the lower (Low; red), middle (Medium; green) and upper (High; blue) thirds of SE distribution. Survival probabilities across groups were compared using the log-rank test, with the corresponding p-value (p). Vertical tick marks show censored patients. The number at risk in each tertile at 0, 200, 400, 600 and 800 days from enrollment is displayed below the plot.